A comparative study for colloidal quantum dot conduction band state calculations

Jun-Wei Luo, Shu-Shen Li, and Jian-Bai Xia

State Key Laboratory for Superlattices and Microstructures,

Institute of Semiconductors, Chinese Academy of Sciences,

P.O. Box 912, Beijing 100083, P.R. China

Lin-Wang Wang*

Computational Research Division, Lawrence

Berkeley National Laboratory, Berkeley, CA 94720

(Dated: September 9, 2005)

Abstract

Via the comparison of the results of a few well controlled calculation methods, we analyze the relative importance of bulk band structure, multi-bulk band coupling and boundary conditions in determining the colloidal quantum dot conduction band eigen energies. We find that while the bulk band structure and correct boundary conditions are important, the effects of multi-bulk band coupling is small. We propose that a heterostructure picture where electron envelope functions inside and outside the quantum dot being connected at the boundary can be applied to colloidal quantum dots.

PACS numbers: 71.15.Dx, 73.22.-f, 81.40.Vw

*Electronic address: lwwang@lbl.gov

Many high quality colloidal semiconductor quantum dots (QDs) [1, 2] of III-V, II-VI, and IV-IV materials have been successfully synthesized by wet chemistry methods. One of the most predominate features of these quantum dots is their size dependent photoluminescence (PL) due to carrier quantum confinement [1, 2]. Many theoretical methods have been used to study this quantum confinement effect. These include the effective mass approximation (EMA) [3]; multi-band $\mathbf{k}\cdot\mathbf{p}$ method [4, 5]; empirical tight-binding method (TB) [6]; empirical pseudopotential method (EPM) [7–10]; and *ab initio* local density approximation (LDA) method [11, 12]. The results of the atomistic methods (TB, EPM, and *ab initio* method) could be very close to each other. For example, if the TB bulk band structure is fitted to the EPM band structure, their calculated QD band gaps are very similar. A recent calculation also indicates that the EPM results are very close to the ab initio LDA results [11]. On the other hand, it is now believed that the simple EMA method often grossly overestimates the quantum confinement effect. There have been comparative studies between the $\mathbf{k}\cdot\mathbf{p}$ results and the EPM results for both colloidal quantum dots [8] and embedded quantum dots [13]. For colloidal quantum dots, it was found that their quantum confinements can be a few hundred meV different, and the order of the valence band states can also be different [8].

While the valence band hole states have been studied extensively in previous comparative studies [8, 13], here we will focus on the conduction band states. Not only the conduction band states contribute more than 70-80% of the total exciton quantum confinement for most semiconductor QDs, the relatively simple characteristics of the conduction band allows us to conduct an in-depth investigation for the causes of the differences between the continuum models and the atomistic model. There are several possible causes: (i) the inadequate description of the bulk band structure in the continuum models [13, 14]; (ii) the neglect of multi-bulk band coupling [7, 13] induced by the quantum dot geometry; and (iii) inadequate boundary conditions of the continuum models [15, 16]. The purpose of this paper is to conduct a controlled analysis of these causes. It will benefit the future development of the continuum models, and will also provide physical insights about the origin of quantum confinement effects. We will focus on the differences between the EMA method and the EPM method. We will study the conduction band minimum (CBM) states, and Si, InAs, InP and CdSe colloidal QDs, which have been calculated previously using EPM methods and their results agree well with experiments [7–10].

The empirical pseudopotential method (EPM) [17] describes the single-particle states ψ_i

and energies E_i in a Schrodinger's equation:

$$(-\frac{1}{2}\nabla^2 + V(\mathbf{r}))\psi_i(\mathbf{r}) = E_i\psi_i(\mathbf{r}), \tag{1}$$

where the total potential $V(\mathbf{r}) = \sum_{\alpha,\mathbf{R}} v_\alpha(\mathbf{r} - \mathbf{R})$ is a direct sum of the screened pseudopotential v_α of the atoms type α, both inside and on the surface of the QD. The bulk atomic pseudopotentials are fitted to the experimental bulk band structure, and the surface pseudopotentials are fitted to remove the band gap states. For InAs, however, instead of using surface passivation atoms, an artificial large band gap barrier material is used to represent the vacuum [7]. Folded spectrum method (FSM) [10] is used to solve the band gap states of Eq.(1).

The EMA models are obtained by taking the effective mass parameters from the EPM bulk band structures. For Si EMA, the inverse effective mass is taken as an average along the three principle directions near the X point. After the effective mass is obtained, a confinement potential $V_{ext}(r)$ will be used to represent a quantum dot. This potential is zero inside the dot, and equals the electron affinity of the EPM in the vacuum barrier region. Outside the QD, the electron is treated as having the same effective mass as inside the QD.

The FSM/EPM and EMA results for the InAs, InP, CdSe, and Si colloidal QDs are shown in Fig.1(a), (b), (c), and (d) respectively. We can see that there is a large difference between the EMA results and the EPM results. EMA results significantly overestimate the quantum confinement effects. In the following, we will trace the sources of this overestimation.

One way to make a clean comparison to the EMA model without the complication of the boundary condition is to add the same EMA $V_{ext}(r)$ to an extended bulk EPM potential $V_b(r)$ [18] in the EPM formalism:

$$(-\frac{1}{2}\nabla^2 + V_b(\mathbf{r}) + V_{ext}(\mathbf{r}))\psi_i(\mathbf{r}) = E_i\psi_i(\mathbf{r}). \tag{2}$$

This is a direct analogous to the EMA QD model. Unfortunately, a direct solution (e.g, using the FSM) for the CBM state of Eq.(2) is usually impossible since V_{ext} outside the QD is larger than the bulk band gap, hence there is no QD band gap in Eq.(2). To yield a sensible CBM solution from Eq.(2), we will use the linear combination of bulk band (LCBB) [19] method. In the LCBB method, the quantum dot state ψ_i is expanded using bulk Bloch

bands $u_{\mathbf{k},n}(\mathbf{r})e^{i\mathbf{k}\cdot\mathbf{r}}$:

$$\psi_i(\mathbf{r}) = \sum_{n}^{N_B} \sum_{\mathbf{k}}^{N_\mathbf{k}} C_{\mathbf{k},n}[u_{\mathbf{k},n}(\mathbf{r})e^{i\mathbf{k}\cdot\mathbf{r}}], \tag{3}$$

where $\mathbf{k}$ is the reciprocal lattice of the supercell and n is the bulk band index. Since the bulk Bloch states are good basis functions of the quantum dot wavefunctions, one can truncate this basis set significantly without introducing big errors compared to the original FSM solved results [19].

Now, if only the first conduction bulk band (n=CB1) is used in Eq.(3), it will yield a QD CBM state in Eq.(2), and the valence band states will be deflated in the effectiv Hamiltonian. The LCBB results solved in this way are shown in Fig.1 as the open squares. They are all higher than the original FSM/EPM CBM of Eq.(1). In the case of InAs and InP, the LCBB result is very different from the EMA result, while for CdSe and Si, and especially for large QDs, the LCBB and EMA results are virtually the same. The difference between LCBB and EMA is due to their bulk band structures [item (i)]. The bulk band structures for InAs, InP, and CdSe near the Γ point are shown in Fig.2(a), (b), and (c) respectively. In the LCBB, since the exact bulk Bloch state is used in the basis set, the exact EPM conduction band band structure is implicitly employed in the calculation. For a 50 Å diameter QD, the corresponding average reciprocal vector k is denoted by the vertical dotted lines in Fig.2(a)-(c). As we can see, at this k, for InAs and InP, there is a big difference between the EMA band structure and the EPM band structure, corroborating their big differences in QD CBM energies. Note that, in a 8x8 k.p model [5, 20], the conduction band energy curve can be much improved upon the single band EMA. But still, for small QD, there could be large differences between the k.p band and the EPM band, especially when other band valleys become important [21].

We now study the multi-bulk band coupling effect induced by the QD geometry. Here, we have to distinguish two different multi-band coupling effects. One is the coupling in a k.p like model, which exists even in bulk at the off Γ k-points. This coupling stems from the fact that the off Γ k-point Bloch state $u_{n,\mathbf{k}}e^{i\mathbf{k}.\mathbf{r}}$ is expanded with the Γ point Bloch state basis $u_{n,\Gamma}e^{i\mathbf{k}.\mathbf{r}}$ in the k.p Hamiltonian. This coupling between $u_{n,\Gamma}$ is needed to get the correct bulk band structure. However, here we are interested in another coupling, which is called here multi-bulk band coupling. This is an coupling (mixing) between the bulk Bloch states $u_{n,\mathbf{k}}e^{i\mathbf{k}.\mathbf{r}}$ for different n's induced by the QD geometry. In the bulk, this coupling is zero. The

amplitude of this coupling determines whether one bulk band is enough to describe the QD conduction band states. To study this coupling, we have included both the bulk conduction band (CB) states and the valence band (VB) states in the LCBB basis of Eq(3) for the InAs quantum dots. The resulting CBM energies are less than 7 meV away from previous CBM energies using one CB band alone in the basis of Eq(3). Besides, if we calculate the total weights for different bulk bands: $W_n = \sum_k^{N_k} |C_{k,n}|^2$, we found that more than 97% of the CBM is from the bulk conduction band, see Fig.2(d). Thus, overall, we found that the effect of multi-bulk band coupling induced by QD geometry is very small.

Since the multi-bulk band coupling effect [item (ii)] is very small, the differences between the one band LCBB results and the direct FSM results shown in Fig.1 must come from the boundary condition treatment [item (iii)]. One possible reason for the CBM energy difference between Eq.(2) (LCBB) and Eq.(1) (FSM) is that in Eq.(2) we have used the same material inside and outside the QD to describe the system. Although the QD/vacuum CB band offsets are the same in Eqs.(1) and (2), the effective mass and bulk Bloch state wavefunction $u_{n,k}$ are very different for vacuum and for the QD in the case of Eq.(1), while they are the same in the case of Eq.(2). On top of this, there is even a qualitative question for whether one can consider the colloidal QD as a heterostructure consisted of the inside QD material and the outside vacuum. For example, what is the role of the surface passivation atoms under this heterostructure picture. An alternative view is to consider the QD as having an infinite wall, so the wavefunction goes to zero at the boundary [3, 4].

To answer these questions, let's first consider what will happen if we set the wavefunction to zero at the boundary. From the effective mass model, it is clear that the energy will go up. This is apparently not the right direction if we want to use it to explain the difference between the one band LCBB results and the FSM results, since the current LCBB results are already higher than the FSM/EPM result. We next consider the effect of different effective masses inside and outside the quantum dot. To this aim, we have solved the EMA model with a different effective masses inside and outside the QD. For outside the QD, the electron effective mass is 1 (except for the InAs QD where the EPM effective mass of 0.787 for the artificial barrier material used). The BenDaniel-Duke boundary condition [22] for the effective mass model is used. The results (EMA2) are shown in Fig.1 as empty triangles. Compared to the original EMA results (where the outside effective mass equals the inside effective mass), the new results have significantly lower the CBM energies. In

fact, they have been lowered so much that the EMA2 now underestimates the confinement energy. The EMA and EMA2 wavefunctions for one CdSe QDs are shown in Fig.2(e). We see that the change of the effective mass in EMA2 allow the wavefunction derivative to have a big discontinuity at the boundary, which relaxes the quantum confinement and lower the confinement energy [23].

The results in Fig.1 and Fig.2 indicate that the effective mass discontinuity at the boundary plays a big role in determine the QD CBM energy. The change of CBM energy from EMA to EMA2 is in the right direction if one uses it to explain the difference between the LCBB and the FSM results in Fig.1. However, quantitatively, it over estimates this correction. That means using effective mass discontinuity alone is not enough, one also needs to consider the fact that the $u_{n,k}$ inside and outside the quantum dot are different. This difference makes the wavefunction connection at the QD boundary difficult, thus potentially will increase the confinement effect, and push the EMA2 results up [16].

Based on the results we found above, we like to propose that a colloidal quantum dot can indeed be considered as a heterostructure system consisted with the inside semiconductor material and the outside vacuum. The role of the surface passivation atoms is just to remove the surface dangling bond states. After these surface states are removed, the edge of band gap states (e.g, CBM) can be treated as normal heterostructure states, with their envelope functions being connected at the surface by some appropriate boundary conditions [15, 16].

In summary, we have systematically studied the difference between the EMA results and the EPM results for the conduction band states of the colloidal QDs. We found that the difference comes mainly from the bulk band structures and the surface boundary conditions. A single band basis will probably be good enough as the multi-bulk band coupling induced by QD geometry is small. In order to get quantitatively accurate results, one has to have exact bulk band structures, and has to take into account the differences between the inside and outside QD effective masses and bulk Bloch states.

This work was supported by the National Natural Science Foundation of China and the special funds for Major State Basic Research Project No. G2001CB309500 of China. The work by L.W. Wang is also funded by U.S. Department of Energy under Contract No.

DE-AC03-76SF00098.

[1] A.P. Alivisatos, Science **217**, 933 (1996).

[2] A. A. Guzelian, U. Banin, A. V. Kadavanich, X. Peng, and A. P. Alivisatos, Appl. Phys. Lett. **69**, 1432 (1996); X. Peng, J. Wickham, and A.P. Alivisatos, J. Am. Chem. Soc. **120**, 5343 (1998); D.S. English, L.E. Pell, Z. Yu, P. F. Barbara, and B. A. Korgel, Nano Lett. **2**, 681 (2002).

[3] T. Takagahara, Phys. Rev. B **47**, 4569 (1993); T. Takagahara and K. Takeda, *ibid.* **53**, R4205 (1996).

[4] A. Mizel, and M.L. Cohen, Solid State Commun. **104**, 401 (1998).

[5] U. Banin, J.C. Lee, A.A. Guzelian, A. V. Kadavanich, A. P. Alivisatos, W. Jaskolski, G.W. Bryant, Al. L. Efros, and M. Rosen, J. Chem. Phys. **109**, 2306 (1998).

[6] S. Lee, L. Jönsson, J.W. Wilkins, G.W. Bryant, and G. Klimeck, Phys. Rev. B **63**, 195318 (2001).

[7] A.J. Williamson and A. Zunger, Phys. Rev. B **61**, 1978 (2000).

[8] H. Fu, L.W. Wang and A. Zunger, Phys. Rev. B **57**, 9971 (1998).

[9] L.W. Wang, and A. Zunger, Phys. Rev. B **53**, 9579 (1993).

[10] L.W. Wang, and A. Zunger, J. Phys. Chem. **98**, 2158 (1994); J. Chem. Phys. **100**, 2394 (1994).

[11] L.W. Wang and J. Li, Phys. Rev. B **69**, 153302 (2004).

[12] S. Öğüt, J.R. Chelikowsky, and S.G. Louie, Phys. Rev. Lett. **79**, 1770 (1997).

[13] L.W. Wang, A.J. Williamson, A. Zunger, H. Jiang, J. Singh, Appl. Phys. Lett. **76**, 339 (2000).

[14] D.M. Wood and A. Zunger, Phys. Rev. B **53**, 7949 (1996).

[15] G.T. Einevoll and L.J. Sham, Phys. Rev. B **49**, 10533 (1994); M.V. Kisin, B.L. Gelmont, and S. Luryi, *ibid.* **58**, 4605 (1998).

[16] M.G. Burt, J. Phys.: Condens. Matter **4**, 6651 (1992).

[17] L.W. Wang and A. Zunger, Phys. Rev. B **51**, 17398 (1995).

[18] J.B. Xia and Y.C Chang, Phys. Rev. B **48**, 5179 (1993).

[19] L.W. Wang and A. Zunger, Phys. Rev. B **59**, 15806 (1999).

[20] Al.L. Efros and M. Rosen, Phys. Rev. B **58**, 7120 (1998).

[21] H. Fu and A. Zunger, Phys. Rev. Lett. **80**, 5397 (1998).

[22] D.J BenDaniel and C.B. Duke, Phys. Rev. **152**, 683 (1966).

[23] G. Bastard, *Wave mechanics applied to semiconductor heterostructures*, (Halsted Press, New York, 1988).

TABLE I: EMA parameters fitted from EPM band structures. E_c is the absolute energy level of the bulk conduction band edge while the vacuum level is zero. It equals the conduction band offset in the EMA QD model.

	CdSe	Si	InP	InAs
m_e^*	0.12	0.263	0.069	0.032
E_c (eV)	-3.50	-3.75	-4.50	-3.92

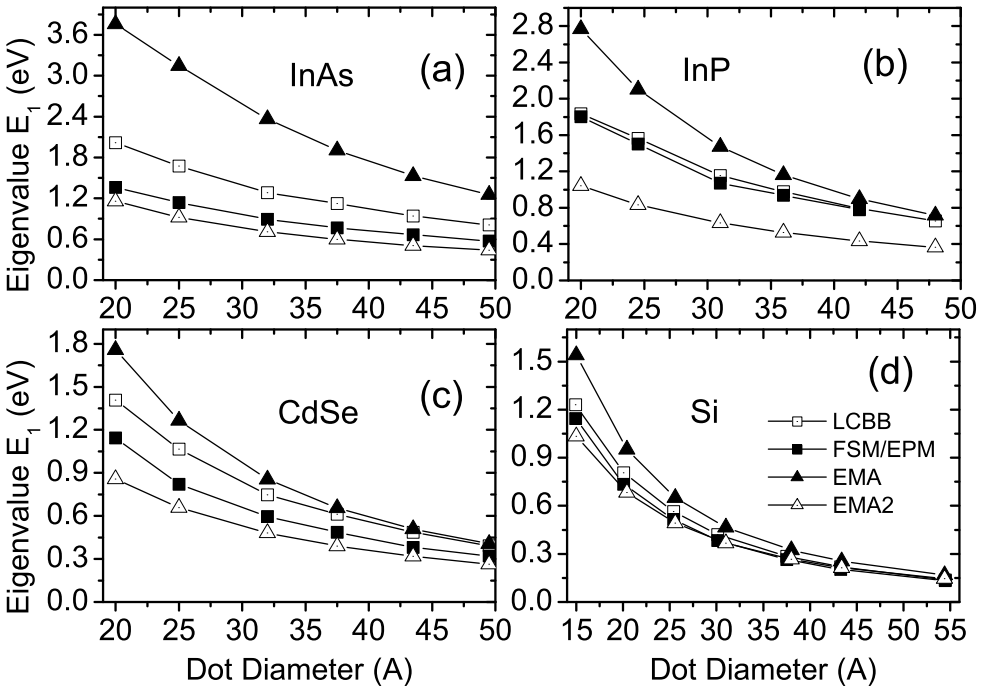

FIG. 1: Conduction band minimum state energies of QDs versus dot diameter using different calculation methods.

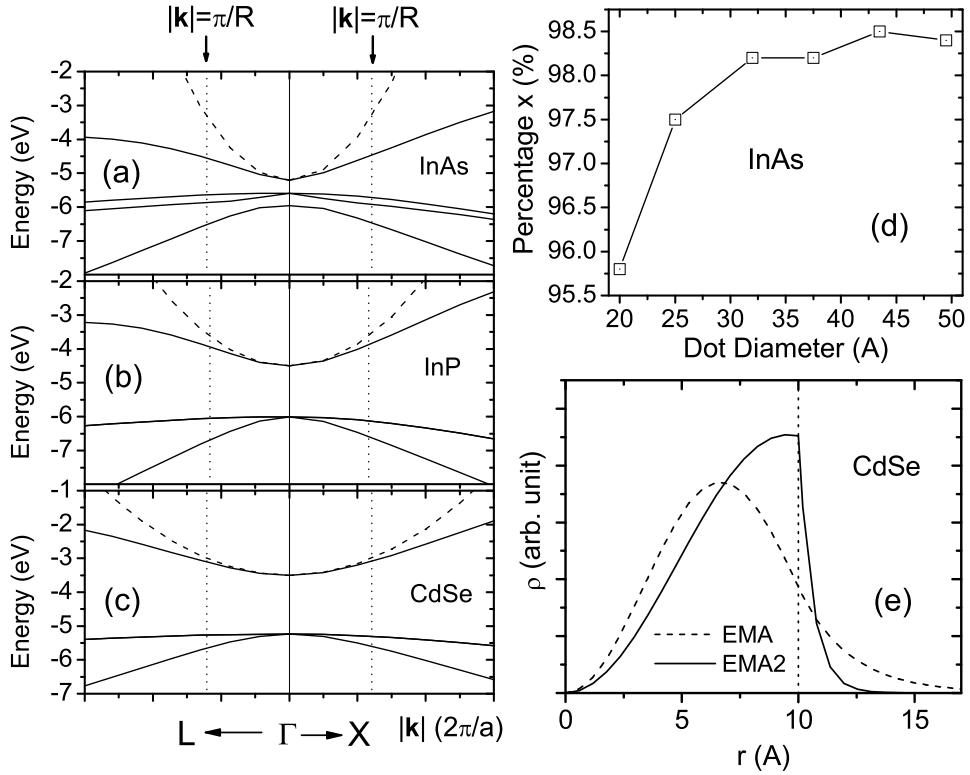

FIG. 2: Band structure of bulk InAs (a), InP (b) and CdSe (c) around Γ point ranged from 0 to 0.3 $(2\pi/a)$ along $\Gamma - X$ and $\Gamma - L$ directions calculated by EPM (solid) and EMA (dashed); (d) The percentage x of lowest electron state of InAs QDs projected onto the bulk InAs conduction band; (e) Radial wavefunction of CdSe QDs with diameter 20 Å for both EMA (dashed) and EMA2 (solid).